Am J Transl Res 2022;14(2):876-887
www.ajtr.org /ISSN:1943-8141/AJTR0139442

Original Article

Klotho/FGF23 and Wnt in SHPT associated with CKD *via* regulating miR-29a

Qing Wu[1], Weifeng Fan[1], Xiaojing Zhong[1], Lihong Zhang[1], Jianying Niu[1], Yong Gu[1,2]

[1]*Department of Nephrology, Shanghai Fifth People's Hospital, Fudan University, Shanghai 200240, China;*
[2]*Department of Nephrology, Huashan Hospital, Fudan University, Shanghai 200240, China*

Received September 27, 2021; Accepted December 10, 2021; Epub February 15, 2022; Published February 28, 2022

Abstract: Objective: Recently, the interaction between Klotho/fibroblast growth factor 23 (FGF-23) axis and Wnt signaling has been recognized to be responsible for chronic kidney disease (CKD)-associated comorbidities, including secondary hyperparathyroidism (SHPT). This study aimed to investigate the molecular mechanism of the interaction between Klotho/FGF23 axis and Wnt. Methods: A SHPT model was successfully established with a high-phosphorus diet plus 5/6 nephrectomy. Cell counting Kit-8 (CCK-8) assay and calcium deposit experiment were applied to detect the proliferation and calcium levels. Quantitative real-time PCR (qRT-PCR), Western blotting and immunofluorescence (IF) were used to determine the expression or location of FGF23, calcification-related factors and β-catenin after lentivirus-mediated Klotho overexpression. Luciferase reporter assay was performed to further validate the transcriptional regulation between microRNA-29a (miR-29a) and Dickkopf-1 (DDK1). Results: We found increased serum biochemical factors including parathyroid hormone (PTH), phosphorus, calcium, enhanced parathyroid calcification, and decreased expressions of Klotho in a rat model of secondary hyperparathyroidism. Moreover, genetic-induced upregulation of Klotho inhibited the proliferation, reduced the calcification and the alkaline phosphatase (ALP) activity, and downregulated Wnt/β-catenin signaling in parathyroid cells. Conclusions: Mechanistically, Klotho suppressed miR-29a expression, led to upregulated expression of Wnt/β-catenin signaling inhibitor DKK1, and finally downregulated the activity of Wnt/β-catenin signaling. These findings suggest a novel molecular mechanism in the pathogenesis of CKD-associated SHPT, which provides a potential therapeutic target in the future.

Keywords: Secondary hyperparathyroidism, Klotho/FGF23 axis, miR-29a, DKK1, Wnt signaling

Introduction

Chronic kidney disease (CKD) often causes metabolic changes, which have an important influence on bone-related mineral metabolism and lead to the deterioration and progress of renal disease and initiation of associated comorbidities [1]. Among these comorbidities, secondary hyperparathyroidism (SHPT) has been recognized as a direct result of CKD and poses a complex alteration in bone and mineral metabolism, which increase the mortality in patients with CKD [2, 3]. SHPT holds the characteristics of hidden onset and quick progress [4]. Thus, identifying patients at risk of developing SHPT is imperative.

As mentioned above, during the development of CKD, changes on bone-related mineral metabolism mainly reflect in increased levels of serum factors including phosphate, calcium, vitamin D, parathyroid hormone (PTH) and metabolic acidosis [5]. Of note, these factors can directly or indirectly increase fibroblast growth factor 23 (FGF-23). For instance, PTH directly affects osteocytes, leading to increased expression of FGF-23 [6]. An oral phosphorus overload can also upregulate FGF-23 expression though controlling the transformation from inorganic phosphate to pyrophosphate in bone [7]. SHPT increases the expression of FGF-23, and such intimate association contributes to the progress of CKD. FGF23 derives mainly from mature osteoblasts which prevents phosphate accumulation during the pathogenesis of CKD *via* increasing urinary phosphorus excretion. This function of FGF23 needs the presence of its specific receptor-FGFR1's co-receptor Klotho in the renal tubules [8]. Until now, it has been well-recognized that Klotho/FGF23 axis serves as a target for kidney treatment as well as a prognostic marker for CKD. Recently, it is found that

aberration of Klotho/FGF23 level is related to modifications in Wnt/β-catenin signaling. PTH can activate Wnt signaling and lead to the increase of FGF-23 expression in osteoblast-like cells [9]. Moreover, the interaction between Klotho/FGF23 axis and Wnt/β-catenin signaling is responsible for CKD-associated comorbidities [10]. However, the interaction between the Klotho/FGF23 axis and Wnt signaling requires more in-depth exploration, particularly in CKD.

As a short (18-25 nucleotides) and highly conserved non-coding RNA molecule, microRNA (miR) directly binds to the 3'-UTR of target mRNAs, and then regulates gene expression at a post-transcriptional level [11]. Accumulating evidence has demonstrated that miRNAs play an important role in a variety of physiological processes, such as cell growth, aging, apoptosis, drug resistance and differentiation [12]. In recent years, it has been revealed that microRNAs can interplay with Wnt/β-catenin pathway at various steps [13]. On the one hand, microRNAs are found to regulate the activation of Wnt/β-catenin pathway; on the other hand, activation of Wnt/β-catenin signaling can upregulate microRNAs expression by directly binding to its promoter. However, the interaction between microRNAs and Wnt/β-catenin pathway in CKD is still unclear. A study found that Wnt/β-catenin signaling played important roles in the pathogenesis of diabetic nephropathy; meanwhile miR-29a was overexpressed, suggesting a possible association between Wnt/β-catenin signaling and miR-29a in CKD and related comorbidities [14]. These studies prompted us to hypothesize that the crosstalk between Klotho/FGF23 axis, Wnt signaling and miR-29a could contribute to the development of CKD-associated SHPT. Better understanding of the regulatory network will provide insight into developing the targeted therapeutic strategies.

In this study, we observed increased serum biochemical factors including intact parathyroid hormone (iPTH), phosphorus, calcium, enhanced parathyroid calcification, and decreased expressions of Klotho in a rat model of secondary hyperparathyroidism. Moreover, the genetic-induced upregulation of Klotho expression inhibited the proliferation, reduced the calcification and the alkaline phosphatase (ALP) activity, and downregulated Wnt/β-catenin signaling in parathyroid cells. Mechanistically, Klotho suppressed the expression of miR-29a, led to upregulated expression of Wnt/β-catenin signaling inhibitor-DKK1, and finally downregulated the activity of Wnt/β-catenin signaling. Altogether, these findings displayed a potential molecular mechanism in the pathogenesis of CKD-associated SHPT, which provided a potential therapeutic target in the future.

Material and methods

SHPT model and histopathological examination

All the animal experiment procedures performed in this study were approved by the Animal Welfare and Ethical Group of Laboratory Animal Science Department, Fudan University (approval number: 2017 1270 A200). Eight-week-old male Sprague Dawley rats were purchased from the Experimental Animal Center, Shanghai Medical School, Fudan University, and maintained in a specific pathogen-free animal facility with a 12 h light/12 h dark cycle and free access to food and water. After one week of adaptive feeding, the rats were randomly divided into 5/6 subtotal nephrectomy group (STNx, n=10) and sham group (n=10). Anesthesia was performed before surgery to relief the pain of animals by peritoneal injection of 1% pentobarbital sodium (40 mg/kg body weight). The 5/6 nephrectomy operation was performed according to a previous study [15]. The sham group only received isolation of the kidney adipose sac without removing kidney tissue. High-phosphorus (HP) diet was given for 8 weeks to establish a model of SHPT. Ten healthy rats at the same age were given a normal-phosphorus (NP) diet for eight weeks as negative control. At the end of the experiment, the rats were sacrificed by peritoneal injection of 120 mg/kg pentobarbital sodium. The serum, kidney and parathyroid samples were collected for further analyses. Serum levels of biochemistry factors including phosphorus (P), calcium (Ca), PTH and serum creatinine (SCr) were measured by enzyme-linked immunosorbent assay (ELISA). Histopathological examination of kidney and parathyroid glands was performed through reviewing HE-staining as well as formalin fixation and paraffin embedding (FFPE) slides. Histological images were taken by using a microscope (Nikon Corporation, Japan).

Cell culture and lentivirus-mediated transfection

Parathyroid tissue was isolated from normal rats. Cell suspension was moved into the dulbecco's modified eagle medium/nutrient mixture F-12 (DMEM/F12)-containing medium for culture (37°C, 5% CO_2). In 5-7 days, cell adherent grew into a monolayer, bordering each other in polyangular shape. Determination of supernatant PTH showed a good secretion function. Cell transfection was performed before experiments. Cells with good growth status were digested with 0.25% trypsin. The number of cells was determined, and cell concentration was controlled, then the cells were seeded into 6-well plates with 100,000 cells per well. Three compound wells were set up in each group. Lentivirus containing Klotho overexpression system, miR-29a mimic or miR-29a inhibitor were constructed by GenePharma Inc. (Suzhou, China). The sequences are as follows: Klotho: ATGCC AGCCCGCGCC CCTCCTCGCC GCCTGCCGCG GCTCTTGCTG; miR-29a mimic: UAGCACCAUCUGAAAUCGGUUA; miR-29a inhibitor: UAACCGAUUUCAGAUGGUGCUA; miR-29a mimic NC: UUCUCCGAACGUGUCACGUTT; miR-29a inhibitor NC: CAGUACUUUUGUGUAGUACAA. Transfection steps were strictly carried out according to the Lipofectamine 2000 instruction. The transfection efficiency of Klotho was validated by Western blotting before the following experiments.

Reagents and antibodies

Klotho MAb (Clone 236214) was purchased from R&D System (Minnesota, USA). Curcumin was purchased from Fluka (Mexico City, Mexico). Cell Counting Kit-8 (CCK-8) was purchased from Dojindo (Kumamoto, Japan). Antibodies against Klotho, FGF-23, runt-related transcription factor 2 (RUNX2) and bone morphogenetic protein-2 (BMP-2) were purchased from Abcam (Cambridge, UK). Antibodies against β-catenin were obtained from Santa Cruz, Inc (Santa Cruz, CA, USA). Fluorescein (FITC)-AffiniPure goat anti-mouse and goat anti-rabbit secondary antibodies were purchased from the Jackson Laboratory (Bar Harbor, ME, USA). 2-(4-amidinophenyl)-1H-indole-6-carboxamidine (DAPI) was purchased from Beyotime (Shanghai, China). Calcium colorimetric assay kit was purchased from Sigma-Aldrich (St. Louis, MO, USA). miRNA qRT-PCR SYBR Kit and FastStart Universal SYBR Green Master kit were purchased from Roche Inc. Lipofectamine 2000 reagent was purchased from Invitrogen (Waltham, MA, USA). The lentivirus containing Klotho overexpression system, the miR-29a mimic, and miR-29a inhibitor were constructed by Gene Pharma Inc. (Suzhou, China).

Quantitative PCR

By using TRIzol Reagent from Invitrogen Inc., total RNA was extracted according to manufacturer's protocols. The expression of miR-29a, Klotho or FGF23 was measured respectively with a miRNA qRT-PCR SYBR Kit and FastStart Universal SYBR Green Master kit from Roche Inc. Data were analyzed according to the classic $2^{-\Delta\Delta Ct}$ method. The primers used in the study were as follows: miR-29a: 5'-TACTGAAC TGTCACGGCAGA-3'(F), 5'-TGTAGTTAG CGACCTCTGCT-3'(R); Klotho: 5'-GAAACCCAAGTCCTCCGCTC-3'(F), 5'-GGGAGGA CACCGCTAAACTC-3'(R); FGF23: 5'-TGGCCATGTAGACGGAACAC-3'(F), 5'-GTAGC CGTTCTCTAGCGTCC-3'(R). β-actin was used as an internal reference.

Western blotting

Proteins were extracted by using radio immunoprecipitation assay (RIPA) buffer containing protease inhibitors and phosphatase inhibitors. Proteins were separated by 10% sodium salt-polyacrylamide gel electrophoresis (SDS-PAGE), and then transferred onto polyvinylidene fluoride (PVDF) membranes. After blocked with 5% bovine serum albumin (BSA) for 1 h, the membranes were, without washing, incubated with anti-Klotho (1:1000), anti-FGF23 (1:1000), anti-RUNX2 (1:1000), anti-BMP2 (1:1000) and anti-β-actin (1:1000) at 4°C overnight. On the second day, the membranes were incubated with horseradish peroxidase (HRP)-conjugated secondary antibodies and visualized with the SuperSignal West Chemiluminescent Substrate Kit from Lifescience Inc. Results were shown after the normalization of the loading amounts in each lane to β-actin. All experiments were performed three times.

Calcium deposit experiment

Calcification of parathyroid gland tissue was determined by calcium deposit experiment, using the calcium colorimetric assay kit. Parathyroid gland tissue was freeze-dried with

0.6 N hydrochloride and decalcified for 24 h. Supernatant calcium was measured by phthalopin colorimetric, and parathyroid gland ca lcium was normalized to dry tissue weight (mmol/g protein). The experiment details followed the manufacturer's protocols [3].

Immunofluorescence (IF)

Cells with or without treatment grew on glass coverslips. After washed in PBS buffer, the cells were fixed by using 4% paraformaldehyde in PBS with pH 7.4 for 15 min at room temperature followed by 0.1% Triton X-100. After being washed for three times, the cells were incubated with 1% BSA and then with the diluted primary antibody (anti-β-catenin, 1:200) in 1% BSA overnight at 4°C. The coverslips were washed three times in PBS, and then incubated with the Fluorescein (FITC)-AffiniPure goat anti-rabbit secondary antibodies for 1 h at room temperature in dark. Cell nuclei were stained with 4',6-diamidino-2'-phenylindole (DAPI) for 5 min at room temperature. Finally, the coverslips were imaged by using Olympus BX51 upright epiFluorescence microscope (Olympus, Tokyo, Japan) at 20× magnification in dark.

Cell proliferation assay

The Cell Counting Kit-8 (CCK-8) was applied to evaluate proliferation of parathyroid cells. Cells were resuspended and seeded into 96-well plates at a density of 5×10^3 cells/well with three replicates. After 12 h, the cells were treated with curcumin at different concentrations (1-20 μM) for 48 h. Subsequently, CCK-8 was added to each well and further incubated at 37°C for 1 h. The absorbance of CCK-8 was detected at 450 nm using a microplate reader (Bio-Rad, Hercules, CA, USA). The experiment was performed in triplicate.

Target prediction and dual-luciferase reporter assay

TargetScan online database was used in order to predict potential target genes for miR-29a (http://www.targetscan.org/vert_71/). Then, the DNA fragment corresponding to the 3'-UTR of Dickkopf-1 (DKK1) mRNA was amplified by PCR assay and inserted into the vector. The 3'-UTR of wild-type DKK1 containing mutant binding site for miR-29a was subcloned by site-directed mutagenesis PCR method. The E-box element at -841 bp was mutated from AUGGCA to AGACGC. Luciferase activity was detected using a dual-luciferase reporter assay system, and the activity of pRL-TK Renilla luciferase was used as an internal control for normalization.

Statistical analysis

Statistical analysis was performed with SPSS 19.0 software (SPSS, Chicago, IL, USA). Quantitative data were reported as the mean ± standard deviation (SD). Student's t-test was used in two-group comparisons. One-way analysis of variance (ANOVA) followed with post-hoc Tukey's test was performed to compare data among multiple groups. Statistical significance was considered when *P*-values were less than 0.05.

Results

Changes of biochemistry factors in SHPT rat model

The rat model of SHPT was successfully established with a high-phosphorus diet plus 5/6 nephrectomy. Histopathological examination of kidney showed compensatory enlargement of the residual kidney, glomerular capillary expansion, mesangial matrix proliferation, a large number of epithelial and endothelial cells necrosis, glomerular fibrosis and sclerosis accompanied by disappearance of capillary cavity at the 28th day postoperatively. Moreover, histopathological examination of the parathyroid glands showed that glands were enlarged, in which cell proliferation showed obvious division, and atypia was sharply accelerated (**Figure 1A**). In addition, the serum levels of biochemistry factors including P, Ca, PTH and SCr were measured by ELISA, and the results showed that serum levels of P, PTH, SCr and Ca were significantly increased in the SHPT model group (STNx+HP), compared to other groups (NC, Sham+HP, STNx+HP, Sham+NP, STNx+NP) (all $P<0.05$; **Figure 1B-E**). Moreover, calcification of parathyroid gland tissues gradually enhanced in SHPT model group (STNx+HP) (**Figure 1F**). Serum level of Klotho was significantly decreased, while serum level of FGF23 was significantly increased in the SHPT group, compared to other groups (all $P<0.05$; **Figure 2A**, **2B**). The mRNA and protein levels of Klotho and FGF23 in dissected parathyroid gland tissues from SHPT rats showed consistent changes with their serum levels (**Figure 2C-F**).

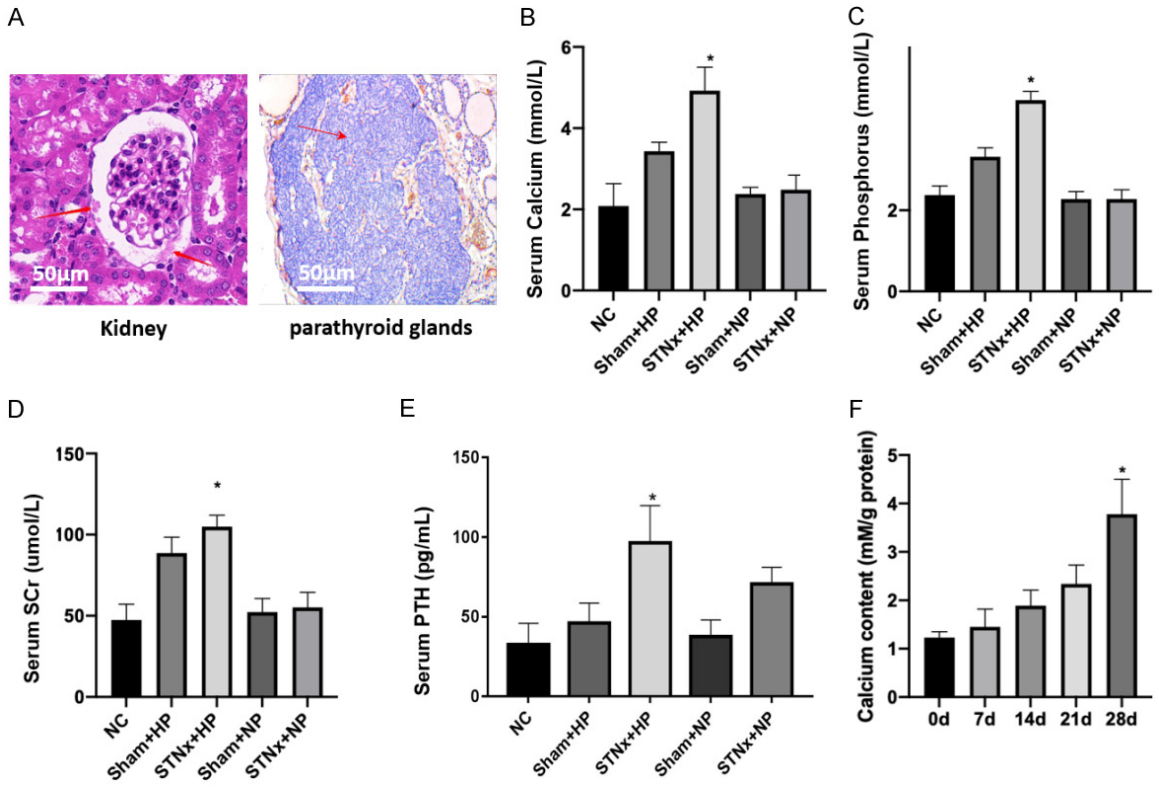

Figure 1. Establishment of SHPT rat model and alteration of serum biochemistry factors including P, Ca, PTH, and SCr in different groups. (A) Representative images of histopathological changes of kidney and parathyroid tissues in SHPT rat model (HE, ×400). Scale bar =50 μm. (Red arrows: The residual glomerular capillary dilatation, mesangial matrix hyperplasia; Parathyroid gland enlargement, with the chief cells mainly distributed and a few oxyphil cells); (B-E) Measured by ELISA, serum levels of P, PTH, and SCr were significantly increased in SHPT model group (STNx+HP), compared to other groups (NC, Sham+HP, STNx+HP, Sham+NP, STNx+NP); (F) Calcification of parathyroid glands tissue was determined with calcium kit. Error bars indicate SEM; n=3. NC: normal control; STNx: 5/6 subtotal nephrectomy; HP: high-phosphorus diet; NP: normal-phosphorus diet; P: phosphorus; Ca: calcium; PTH: parathyroid hormone; SCr: serum creatinine; SHPT: secondary hyperparathyroidism; ELISA: enzyme-linked immuno sorbent assay. Data were analyzed by one-way ANOVA with Tukey's test for multiple comparisons. *P<0.05 *vs*. the NC group (B-E). *P<0.05 *vs*. the 0 d (F).

Klotho overexpression suppressed the expression of miR-29a in parathyroid cells

The findings above encouraged us to explore the role of Klotho/FGF23 axis in the pathogenesis of SHPT, hence lentivirus-mediated overexpression of Klotho was transfected into parathyroid cells (**Figure 3A**, **3B**). It was found that Klotho overexpression inhibited the secretion of PTH in parathyroid cells (**Figure 3G**), expressions of calcification-related factors (RUNX2 and BMP2; **Figure 3C**, **3D**) and nuclear translocation of β-catenin (**Figure 3E**, **3F**), but upregulated the expression of FGF23 (**Figure 3C**, **3D**). Moreover, Klotho overexpression inhibited the proliferation, reduced the calcification, and suppressed the ALP activity of parathyroid cells (**Figure 3H-J**). Notably, Klotho overexpression also suppressed miR-29a expression in parathyroid cells, as expected (**Figure 3K**). Furthermore, we added Klotho protein into the media and found that miR-29a expression was suppressed in parathyroid cells (**Figure 3L**). Taken together, these results suggest that the miR-29a expression is regulated by Klotho during the pathogenesis of parathyroid cells.

miR-29a directly targeted DKK1 in parathyroid cells

As mentioned above, the interplay between Klotho/FGF23 axis and Wnt/β-catenin signaling contributes to the development of CKD-associated comorbidities [10]. Meanwhile, the WNT-β-catenin pathway is negatively regulated by DKK-1 through competitive binding of

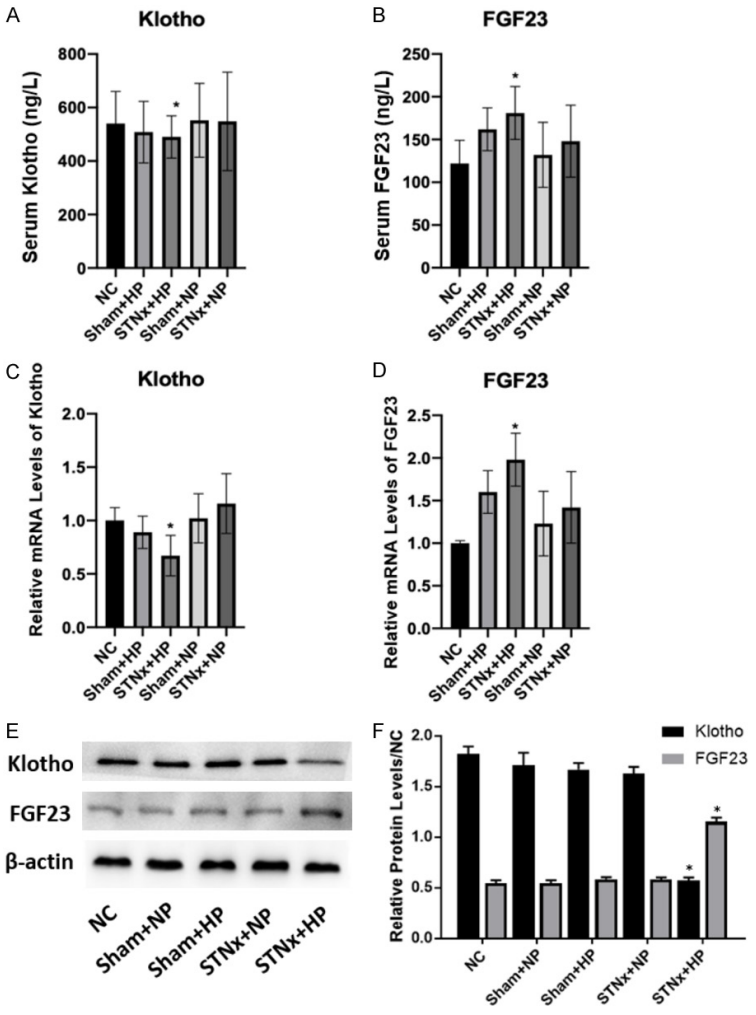

Figure 2. Expressions of Klotho and FGF23 in a variety of groups. (A, B) Serum level of Klotho and FGF23 was measured by ELISA; (C-F) The mRNA and protein levels of Klotho (C, E, F) and FGF23 (D-F) in dissected parathyroid glands tissue. Error bars indicate SEM; n=3. NC: normal control; STNx: 5/6 subtotal nephrectomy; HP: high-phosphorus diet; NP: normal-phosphorus diet; FGF23: fibroblast growth factor 23. Data were analyzed by one-way ANOVA with Tukey's test for multiple comparisons. *P<0.05 *vs.* the NC group.

LRP5/6 or forming a ternary complex with kremen and LRP5/6 [16]. To further explore the relationship of miR-29a with DKK-1 and the inhibitor of Wnt/β-catenin pathway in parathyroid cells, we screened the targets of miR-29a and identified DKK-1 as a potential target (**Figure 4A**). Then, we found that after co-transfection of miR-29a mimics, the luciferase activity decreased in cells transfected with wild-type DKK1 3'-UTR; in contrast, the activity relatively increased in cells co-transfected with miR-29a inhibitors and wild-type DKK1 3'-UTR. Overexpression and down-regulation of miR-29a had no significant effect on the luciferase activity in cells transfected with mutant DKK1 3'-UTR (**Figure 4B**). Moreover, we found that miR-29a mimics significantly decreased DKK-1, but miR-29a inhibitors significantly increased DKK-1 (**Figure 4C-E**). These findings verified the hypothesis that miR-29a negatively regulated DKK-1 expression at a transcriptional level in parathyroid cells.

Inhibiting expression of miR-29a by Klotho regulated the Wnt/β-catenin signaling via increasing DKK-1 expression in parathyroid cells

To verify the effect of miR-29a on the activation of Wnt/β-catenin signaling, we observed the nuclear translocation of β-catenin parathyroid cells transfected with miR-29a mimics, inhibitors or control. The results showed that nuclear β-catenin was increased in parathyroid cells transfected with miR-29a mimics, whereas nuclear β-catenin was decreased in parathyroid cells transfected with miR-29a inhibitors (**Figure 5A**, **5B**). Meanwhile, the secretion of PTH, calcification and proliferation were increased in parathyroid cells transfected with miR-29a mimics while decreased in parathyroid cells transfected with miR-29a inhibitors, compared to the controls (**Figure 5C-E**). To further investigate whether the role of Klotho in regulating Wnt/β-catenin signaling depends on miR-29a, we added soluble Klotho protein into culture media of parathyroid cells transfected with miR-29a mimics. It was found that compared to the controls, nuclear β-catenin was relatively increased but DKK-1 expression was decreased (**Figure 5F-I**), and the secretion of PTH, calcification and proliferation were also increased (**Figure 5J-L**).

Discussion

SHPT is a common complication in patients with CKD. With the decline of glomerular filtration rate, the incidence of SHPT is gradually

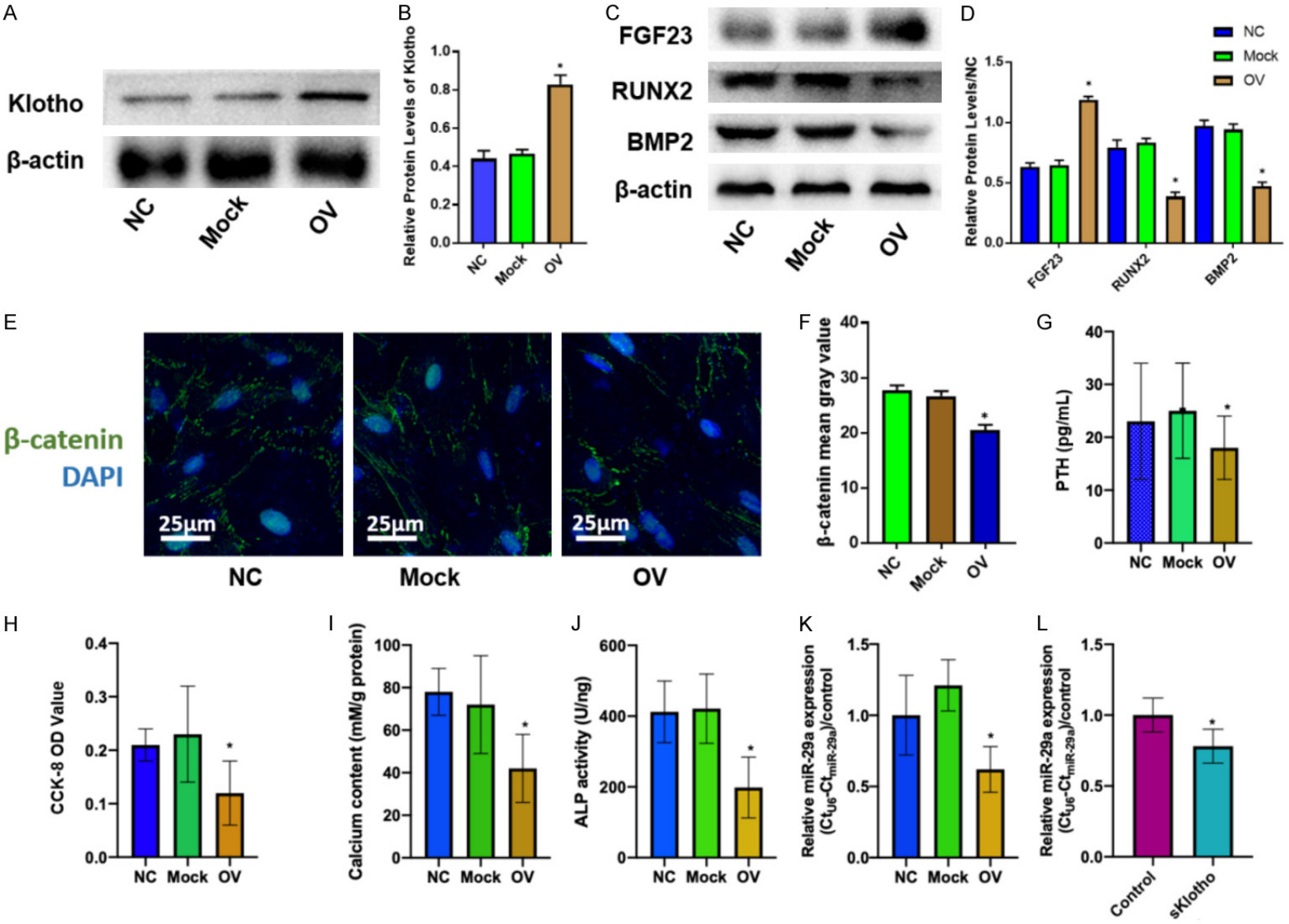

Figure 3. Klotho overexpression suppressed the expression of miR-29a in parathyroid cells. (A, B) Lentivirus-mediated overexpression construct of Klotho was performed; (C, D) Expressions of calcification-related factors (RUNX2 and BMP2) were determined by WB; (E, F) Nuclear translocation of β-catenin was imaged by IF (×1000), scale bar =25 μm; (G) The secretion of PTH in parathyroid cells was measured by ELISA; (H) The cell proliferation was performed by CCK-8 assay; (I) The

calcification was measured by calcium kit; (J) The ALP activity of parathyroid cells was measured by ELISA. (K, L) miR-29a expression in parathyroid cells was determined by qPCR. Error bars indicate SEM; n=3. NC: normal control; Mock: blank control; OV: Klotho over expression; PTH: parathyroid hormone; ALP: alkaline phosphatase; RUNX2: anti-RUNX family transcription factor-2; BMP-2: anti-bone morphogenetic protein-2; ELISA: enzyme-linked immuno sorbent assay; WB: western blotting; qPCR: quantitative PCR; IF: immunofluorescence; II counting kit-8; miR-29a: microRNA-29a. Data in (B, D and F-K) were analyzed by one-way ANOVA with Tukey's test for multiple comparisons. *P<0.05 *vs*. the NC group. Data in (L) were analyzed by Student's t-test, *P<0.05 *vs*. the control group.

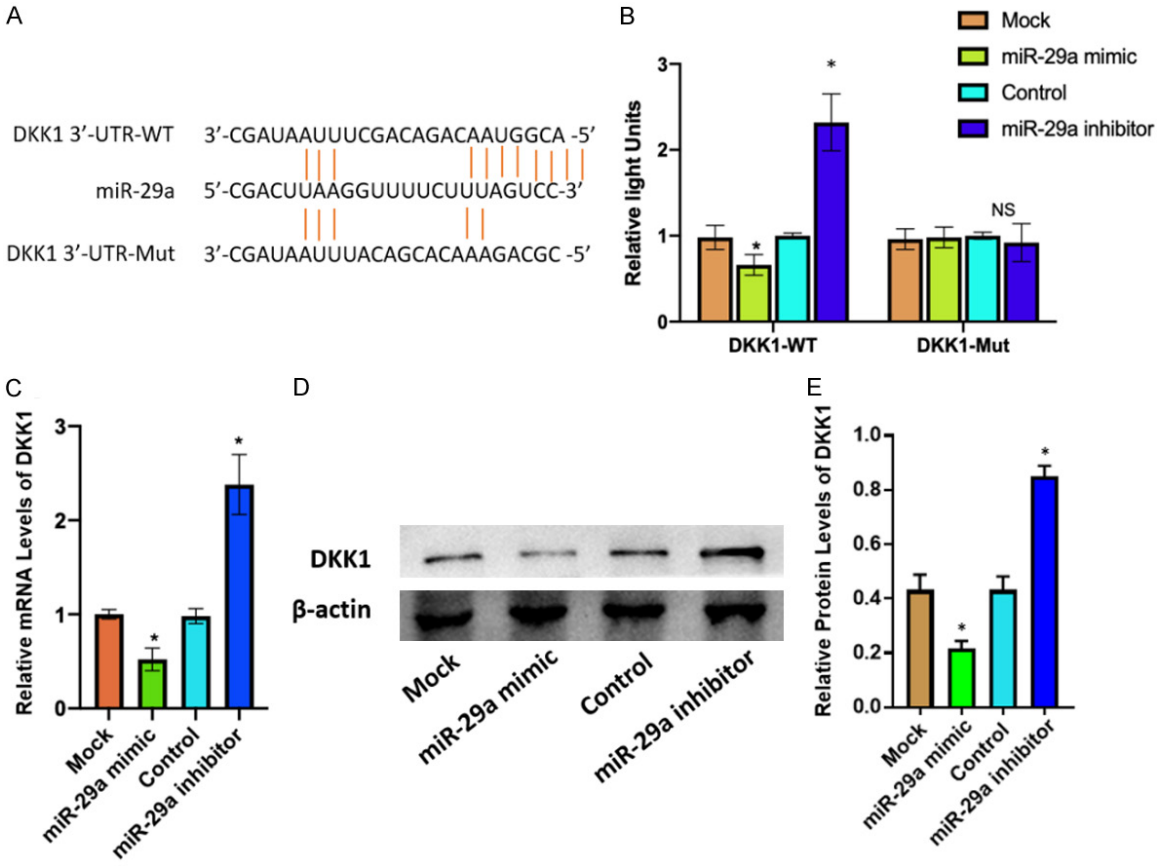

Figure 4. miR-29a directly targeted DKK1 and regulated the Wnt/β-catenin signaling. A. Schematic representation of the putative target site for miR-29a in the 3'-UTR of DKK1; B. Predicted wild-type (WT) or mutated (Mut) 3'-UTR of DKK1 gene; the activity was assessed by luciferase reporter gene assay; C. In parathyroid cells, relative mRNA levels of DKK1 were measured by quantity PCR; D, E. DKK1 protein was detected by western blotting. Error bars indicate SEM; n=3. miR-29a: microRNA-29a; DKK1: Dickkopf-1. B, C, E. Data were analyzed by one-way ANOVA with Tukey's test for multiple comparisons. *P<0.05 *vs*. the control group.

increased [17]. SHPT is characterized by hyperplasia of parathyroid glands and excessive synthesis and secretion of PTH. As a result, excessive PTH can cause the enhancement of bone resorption and changes of calcium and phosphorus metabolism, finally leading to serious complications such as vascular calcification and cardiovascular disease [3]. The pathogenesis of SHPT is related to a variety of factors, including high blood phosphorus, low blood calcium, deficiency of active vitamin D, malabsorption of intestinal calcium, downregulation of parathyroid vitamin D receptor (VDR) and calcium sensitive receptor (CaSR) expression, and alteration of transcription levels of the PTH gene [18]. In recent years, studies on the role of fibroblast growth factor-23 (FGF-23)/Klotho and its downstream signal pathways in the pathogenesis of SHPT have attracted more and more attentions. Mounting *in vivo* and *in vitro* experiments have demonstrated that in physiological conditions, FGF-23 inhibits PTH secre-

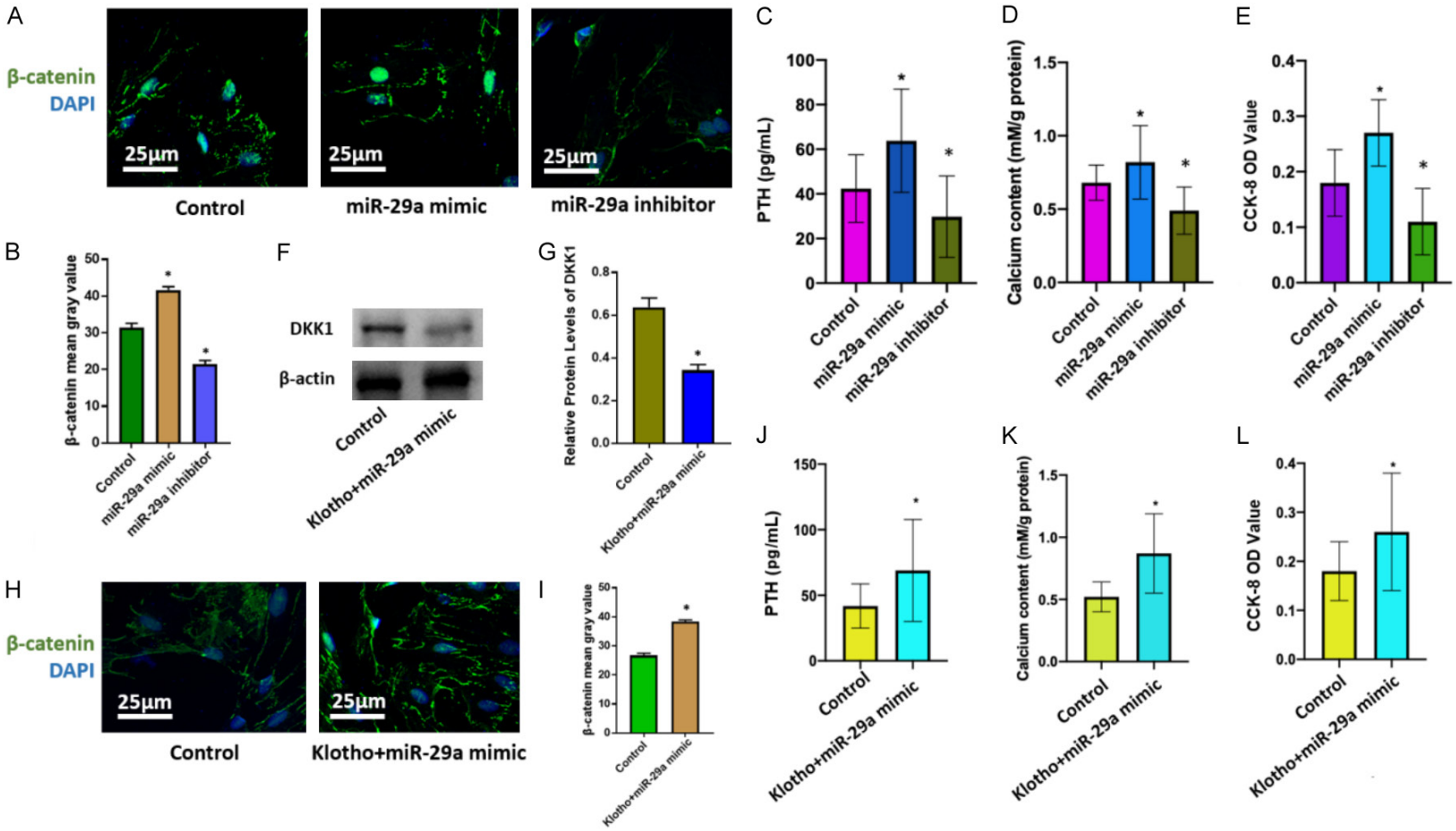

Figure 5. Suppressed expression of miR-29a by Klotho regulated the Wnt/β-catenin signaling via increasing DKK-1 expression in parathyroid cells. A, B. The nuclear translocation of β-catenin in parathyroid cells was presented by IF assay (×1000), Scale bar =25 μm; C-E. The secretion of PTH, calcification and proliferation in parathyroid cells were determined in cells; F-I. DKK-1 expression was measured by western blotting, and nuclear β-catenin was measured by IF (×1000), scale bar =25 μm; J-L. The secretion of PTH, calcification and proliferation were measured by the according kits. Error bars indicate SEM; n=3. miR-29a: microRNA-29a; DKK1: Dickkopf-1. IF: immunofluorescence; PTH: parathyroid hormone. B-E. Data were analyzed by one-way ANOVA with Tukey's test for multiple comparisons. *P<0.05 *vs*. the control group. G, I-L. Data were analyzed by Student's t-test, *P<0.05 *vs*. the control group.

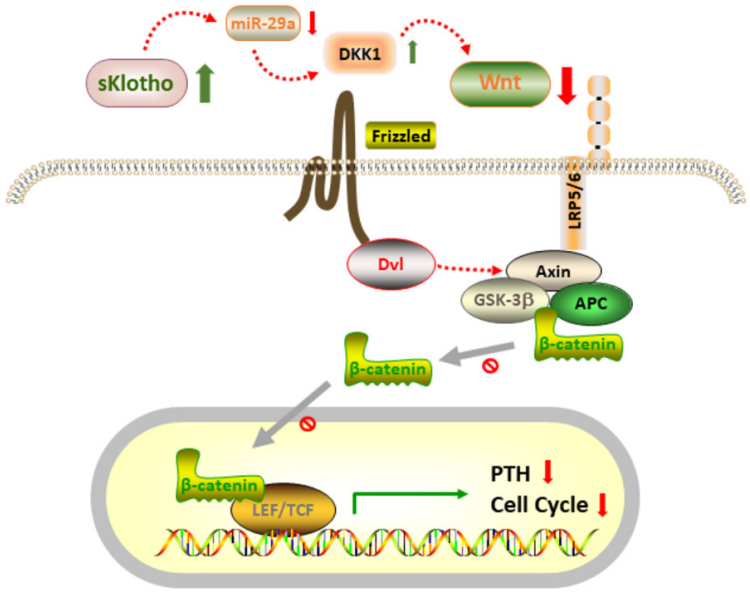

Figure 6. Regulation of Wnt/β-catenin signaling by Klotho *via* miR-29a-targeted DKK-1 expression in parathyroid cells.

tion by combining with the Klotho-FGFRI complex on the parathyroid cell membrane to activate the intracellular mitogen-activated protein kinase (MAPK) signal transduction pathway [19]. However, when CKD is accompanied by SHPT, the PTH level remains high even if FGF23 is at a high level [20]. Current research has shown that FGF23 inhibits PTH production at various steps that can cause parathyroid cells to resist the regulation of FGF23 and finally cause SHPT [21]. In fact, the increase in FGF23 levels is accompanied by a marked decrease in Klotho, with progressive changes in the parameters of mineral metabolism during CKD progression; parallelly, there are also changes in the levels of Wnt inhibitors, such as Dickkopf-related proteins [22]. However, the interaction between the FGF23/Klotho and Wnt signaling has not been fully revealed until now. In this study, we successfully established a rat model of SHPT with a high-phosphorus diet plus 5/6 nephrectomy, which displayed classical histopathological manifestations and the increase of serum P, PTH, SCr as well as the decrease of serum Ca. The model provided a good study platform for subsequent experiments.

It has been well-known that FGF23 can inhibit $1,25(OH)_2D$ and PTH production in the late-stage of CKD; meanwhile, the increase of the FGF23 level is often accompanied by a marked decrease in Klotho level. In our study, we also observed the decrease of Klotho and simultaneous increase of FGF23 in the SHPT rat model. The finding was consistent with previous studies [23, 24]. Although there are still controversies, a direct participation of the FGF23/Klotho axis in the pathogenesis of CKD and its associated complications has been recognized. The *klotho* gene is situated on the large arm of the human chromosome 13 and is expressed mostly in kidney tubules, parathyroid glands and choroid plexus [25]. Klotho expression is induced by VDR activators, thus, Klotho plays a key role in the FGF23-mediated effects on mineral metabolism. It was reflected in the finding "Klotho overexpression reduced the calcification, and inhibited the ALP activity in parathyroid cells". Furthermore, Klotho overexpression inhibited the secretion of PTH and nuclear translocation of β-catenin but upregulated the expression of FGF23 in parathyroid cells, which suggested the importance of Klotho in the pathogenesis of SHPT.

Some of the mechanisms in regulating FGF23/Klotho levels have been verified to be related to modifications in the Wnt signaling. Meanwhile, FGF23/Klotho axis and Wnt signaling can interplay vice versa and may form a feedback loop in CKD-related complications [10]. However, the relationship between FGF23/Klotho and Wnt signaling in SHPT is not fully revealed. Recently, various miRNAs have been reported to be involved in the biological process of CKD [26]. Aberrant expression of miRNAs is closely associated with vascular calcification and fibrosis through regulating post-transcriptional mechanisms of PTH gene expression and parathyroid cells activation [18, 27, 28]. In this study, we found that miR-29a was downregulated in parathyroid cells when Klotho is overexpressed. It was demonstrated that downregulation of miR-29a was associated with CKD through suppressing myogenesis [29]. The results encouraged us to explore whether miR-29a participates in the pathogenesis of SHPT. Then, we found that Klotho overexpression also suppressed miR-29a expression in parathyroid

cells, suggesting a possible role of miR-29a in the pathogenesis of SHPT. However, the molecular mechanism of how Klotho regulates miR-29a in parathyroid cells was not revealed in the current study. Nevertheless, we gained a novel finding that miR-29a directly targeted DKK1, a negative regulator of Wnt signaling in parathyroid cells. A variety of ligands, receptors and coreceptors orchestrate Wnt signaling, which can be regulated at different levels. Among these modulators, DKK1 is well characterized [30]. In the study, we further demonstrated that Klotho regulated Wnt/β-catenin signaling depending on miR-29a, and finally led to alterations in the secretion of PTH, expressions of calcification-related factors (RUNX2 and BMP2) and proliferation in parathyroid cells (**Figure 6**).

This study was conducted at an animal and a cellular level, and the relevant results need to be further verified in the parathyroid tissue of patients with SHPT. Due to the limitation of the experimental conditions, there was no commercialized SHPT cell line, and cell transfection was unable to proceed in the tissue culture of patients with hyperparathyroidism, so this study was conducted in normal rat parathyroid cells.

Altogether, based on these results, we concluded that the suppressed expression of miR-29a by Klotho regulated the Wnt/β-catenin signaling *via* increasing DKK1 expression in parathyroid cells. Currently, clinical trials of miR-based therapeutic agents are ongoing for CKD and associated complications. As to CKD-associated SHPT, more challenges still exist because of insufficient understanding of its pathogenesis. Our study, for the first time, demonstrated the crosstalk between Kloth/FGF23 axis and Wnt/β-catenin signaling through miR-29a inhibiting DKK-1. The regulatory network presents a better understanding of SHPT pathogenesis and provides insight into miR-based therapeutic development for SHPT in the future.

Acknowledgements

This work was supported by the Special funds for Clinical Medical Research of Chinese Medical Association (17010040673), High-level Professional Physician Training Program of Minhang District (2020MZYS13) and Minhang District Natural Science Foundation (2016-MHZ09).

Disclosure of conflict of interest

None.

Address correspondence to: Yong Gu and Jianying Niu, Department of Nephrology, Shanghai Fifth People's Hospital, Fudan University, No. 801 Heqing Road, Shanghai 200240, China. Tel: +86-021-24289329; E-mail: yonggu_hs@163.com (YG); jianyingniu_wy@163.com (JYN)

References

[1] Webster AC, Nagler EV, Morton RL and Masson P. Chronic kidney disease. Lancet 2017; 389: 1238-1252.
[2] Messa P and Alfieri CM. Secondary and tertiary hyperparathyroidism. Front Horm Res 2019; 51: 91-108.
[3] Galassi A, Ciceri P, Fasulo E, Carugo S, Cianciolo G and Cozzolino M. Management of secondary hyperparathyroidism in chronic kidney disease: a focus on the elderly. Drugs Aging 2019; 36: 885-895.
[4] Komaba H, Kakuta T and Fukagawa M. Management of secondary hyperparathyroidism: how and why? Clin Exp Nephrol 2017; 21 Suppl 1: 37-45.
[5] Bover J, Bailone L, López-Báez V, Benito S, Ciceri P, Galassi A and Cozzolino M. Osteoporosis, bone mineral density and CKD-MBD: treatment considerations. J Nephrol 2017; 30: 677-687.
[6] Khundmiri SJ, Murray RD and Lederer E. PTH and vitamin D. Compr Physiol 2016; 6: 561-601.
[7] Richter B and Faul C. FGF23 actions on target tissues-with and without klotho. Front Endocrinol (Lausanne) 2018; 9: 189.
[8] Rodríguez M. FGF23: is it another biomarker for phosphate-calcium metabolism? Adv Ther 2020; 37 Suppl 2: 73-79.
[9] Glosse P, Fajol A, Hirche F, Feger M, Voelkl J, Lang F, Stangl GI and Föller M. A high-fat diet stimulates fibroblast growth factor 23 formation in mice through TNF-α upregulation. Nutr Diabetes 2018; 8: 36.
[10] Muñoz-Castañeda JR, Rodelo-Haad C, Pendon-Ruiz de Mier MV, Martin-Malo A, Santamaria R and Rodriguez M. Klotho/FGF23 and Wnt signaling as important players in the comorbidities associated with chronic kidney disease. Toxins (Basel) 2020; 12: 185.
[11] Mohr AM and Mott JL. Overview of microRNA biology. Semin Liver Dis 2015; 35: 3-11.
[12] Gowen AM, Odegaard KE, Hernandez J, Chand S, Koul S, Pendyala G and Yelamanchili SV. Role of microRNAs in the pathophysiology of

addiction. Wiley Interdiscip Rev RNA 2021; 12: e1637.
[13] Rana MA, Ijaz B, Daud M, Tariq S, Nadeem T and Husnain T. Interplay of Wnt β-Catenin pathway and miRNAs in HBV pathogenesis leading to HCC. Clin Res Hepatol Gastroenterol 2019; 43: 373-386.
[14] Tung CW, Hsu YC, Shih YH, Chang PJ and Lin CL. Glomerular mesangial cell and podocyte injuries in diabetic nephropathy. Nephrology (Carlton) 2018; 23 Suppl 4: 32-37.
[15] Ni LH, Tang RN, Lv LL, Wu M, Wang B, Wang FM, Ni HF, Song KY, Wang LT, Meng Z, Chen Q and Liu BC. A rat model of SHPT with bone abnormalities in CKD induced by adenine and a high phosphorus diet. Biochem Biophys Res Commun 2018; 498: 654-659.
[16] Schunk SJ, Floege J, Fliser D and Speer T. WNT-β-catenin signalling-a versatile player in kidney injury and repair. Nat Rev Nephrol 2021; 17: 172-184.
[17] Alfieri C, Regalia A, Zanoni F, Vettoretti S, Cozzolino M and Messa P. The importance of adherence in the treatment of secondary hyperparathyroidism. Blood Purif 2019; 47: 37-44.
[18] Kilav-Levin R, Hassan A, Nechama M, Shilo V, Silver J, Ben-Dov IZ and Naveh-Many T. Post-transcriptional mechanisms regulating parathyroid hormone gene expression in secondary hyperparathyroidism. FEBS J 2020; 287: 2903-2913.
[19] Silver J and Naveh-Many T. FGF23 and the parathyroid. Adv Exp Med Biol 2012; 728: 92-99.
[20] Cannata-Andía JB, Martín-Carro B, Martín-Vírgala J, Rodríguez-Carrio J, Bande-Fernández JJ, Alonso-Montes C and Carrillo-López N. Chronic kidney disease-mineral and bone disorders: pathogenesis and management. Calcif Tissue Int 2021; 108: 410-422.
[21] Lu CL, Yeih DF, Hou YC, Jow GM, Li ZY, Liu WC, Zheng CM, Lin YF, Shyu JF, Chen R, Huang CY and Lu KC. The emerging role of nutritional vitamin d in secondary hyperparathyroidism in CKD. Nutrients 2018; 10: 1890.
[22] Drüeke TB. Hyperparathyroidism in chronic kidney disease. In: Drüeke TB,editor. South Dartmouth (MA); 2000.
[23] Chen XJ, Chen X, Wu WJ, Zhou Q, Gong XH and Shi BM. Effects of FGF-23-mediated ERK/MAPK signaling pathway on parathyroid hormone secretion of parathyroid cells in rats with secondary hyperparathyroidism. J Cell Physiol 2018; 233: 7092-7102.
[24] Naveh-Many T and Volovelsky O. Parathyroid cell proliferation in secondary hyperparathyroidism of chronic kidney disease. Int J Mol Sci 2020; 21: 4332.
[25] Erben RG and Andrukhova O. FGF23-klotho signaling axis in the kidney. Bone 2017; 100: 62-68.
[26] Peters LJF, Floege J, Biessen EAL, Jankowski J and van der Vorst EPC. MicroRNAs in chronic kidney disease: four candidates for clinical application. Int J Mol Sci 2020; 21: 6547.
[27] Ryu J, Ahn Y, Kook H and Kim YK. The roles of non-coding RNAs in vascular calcification and opportunities as therapeutic targets. Pharmacol Ther 2021; 218: 107675.
[28] Ruiz-Ortega M, Rayego-Mateos S, Lamas S, Ortiz A and Rodrigues-Diez RR. Targeting the progression of chronic kidney disease. Nat Rev Nephrol 2020; 16: 269-288.
[29] Wang XH, Hu Z, Klein JD, Zhang L, Fang F and Mitch WE. Decreased miR-29 suppresses myogenesis in CKD. J Am Soc Nephrol 2011; 22: 2068-2076.
[30] Baetta R and Banfi C. Dkk (Dickkopf) proteins. Arterioscler Thromb Vasc Biol 2019; 39: 1330-1342.